

NUMERICAL SIMULATION OF AN IMPACT-GENERATED STRESS-GLUT FIELD AND CORRESPONDING SEISMIC SOURCE. M. Froment^{1,2}, P. Lognonné¹, C. Larmat², E. Rougier², Z. Lei², T. Kawamura¹ and F. Karakostas³. ¹Université de Paris, Institut de Physique du Globe de Paris, CNRS, Paris, France, mfroment@ipggp.fr, ²Earth and Environmental Sciences Division 17, Los Alamos National Laboratory, Los Alamos, NM, USA, ³Department of Geology, University of Maryland, MD, College Park, USA.

Introduction: Meteorite impacts are a known seismic source on the Moon [1,2] and the Earth [3]. Although no detection was performed yet [4], impacts are also thought to be a potential source of seismic signal on Mars, now equipped with a seismometer as part of the InSight mission [5]. In order to improve the exploitation of impact-generated signals for planetary seismology studies, better models of their seismic source are needed. These models should be able to relate the properties of an impactor (velocity, angle, mass and composition) and its target (material response, seismic velocities) to the amplitude and spectral features of seismic waves in the far-field.

A common simplification in seismology consists in considering the source of far-field signal to be a sum of force monopoles and dipoles radiating from a point in space [6]. This source is represented mathematically by a time-varying force vector and moment tensor.

Here, we present a numerical method to compute the point source (i.e., the moment tensor and single force) generated by an impact on a planetary surface, based on the shock code HOSS [7,8,9]. We simulate shock-induced stress and velocity fields in 3D, from which the “stress glut” field [10] and momentum transfer from impactor to target are deduced. Simulation results also provide information on the source dimensions in space and main damage mechanisms.

Point Source Theory and Stress Glut: A seismic event occurs when inelastic processes bring a medium initially at elastic equilibrium to a new state. The source can be described by the change of physical quantities in the near-field over the duration of the event. In that way, the notion of “stress glut” was introduced by Backus & Mulcahy (1976) [10], to describe both transient and permanent inelastic processes in the source region based on the stress evolution. Their study led to the first analytical expression of an earthquake seismic moment M_{ij} , as the volume integral of the Stress Glut Π_{ij} .

$$M_{ij}(t) = \int_{V(t)} \Pi_{ij}(t) dV. \quad (1)$$

Later, a similar method was used by Lognonné et al. (1994) [11] to determine the seismic moment of an impact in a fluid medium. Here, in the case of an impact occurring in a solid elastic medium, the 6-component stress glut tensor can be expressed in cartesian coordinates by:

$$\Pi_{ij}(t) = (\Psi_{ij,Elastic} - \Psi_{ij,True} + \rho v_i v_j)(t) \quad (2)$$

where Ψ stands for the elastic and true stress tensors mentioned in [10], v is the velocity and ρ the density in the impacted medium. The first two terms in equation (2) represent inelasticity, while the last term is related to material advection. We also compute the momentum brought by the impactor to the target, from which the single force is derived:

$$F_i(t) = \int_{V(t)} \rho_0 \frac{dv_i}{dt}(t) dV. \quad (3)$$

Numerical Method for Stress Glut computation:

Calculation of the advection term of (2) is straightforward. In order to measure the inelastic term, we use two different HOSS material models for the volumetric and deviatoric deformation of the simulated target. The volumetric deformation is based on a porous equation of state described in [12], while the algorithm to calculate deviatoric strains is reported in [13].

Volumetric Stress Glut. HOSS provides a measure of pressure according to volumetric strain in the simulated material. Up to a certain point in pressure and strain, the material responds elastically. Beyond this point, pore-crush and plasticity occur. The difference between the calculated pressure and the ideal elastic pressure is the volumetric stress glut (or pressure glut).

Deviatoric Stress Glut. Deviatoric stresses are derived from a decomposition of deformation into different modes. At each timestep, the evolution of stresses is predicted based on an elastic relationship. Then a return mapping algorithm is introduced to correct the stress state if it is outside of the material’s yield surface. In this approach, the deviatoric terms of the stress glut tensor are thus simply equal to the accumulation of this stress correction.

Simulation of the Stress Glut field. In HOSS, stresses and velocity fields are simulated using an unstructured grid of tetrahedral elements, and stress glut is computed for each element. Results are output with a chosen frequency in the form of 3D fields, from which volume integrals can be performed.

We test this method with an impact simulation on a 45° cylindrical sector, 15 m in radius and depth, totaling 750,000 elements. The impactor is a 10 cm-radius 45° basaltic sphere sector with a 1 km/s vertical velocity and mass of 1.5 kg, simulated with a Tillotson equation of state [14]. The target is composed of sand with 44% porosity adapted from [15], simulated with the material models mentioned above.

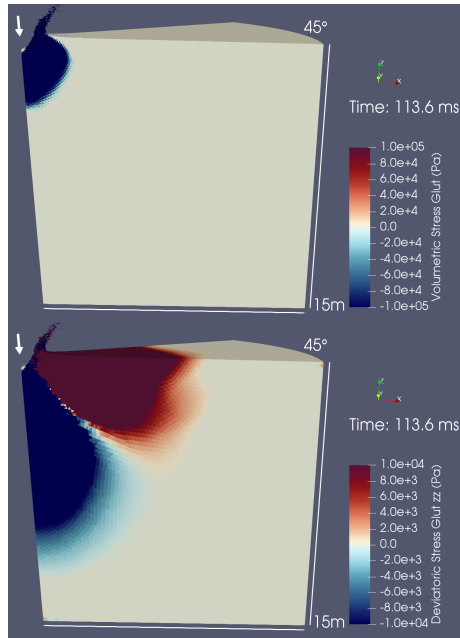


Figure 1: Volumetric (top) and vertical deviatoric (bottom) stress glut field (advection term ignored) generated by a 1000m/s HOSS impact simulation, after 113.6ms. Blue regions identify areas where elements were permanently compressed in volume (top) and in the z-direction (bottom), while red areas illustrate a permanent vertical extension.

Results: The simulation was run up to 113.6ms. The computed pressure glut field and the Π_{zz} component of the stress glut field without the advection term of equation (2), are shown on Figure [1]. The limits of the region of inelasticity created by the impact is thus visible. The point source parameters are derived from the integral of the stress glut and the momentum transfer after using cylindrical symmetry to extrapolate the result of the 45° modeling sector into a full 360° field. Figure [2] shows a peak value in force of $F_z = -2.6 \cdot 10^7$ N, and for the moment components of $M_{zz} = -8.3 \cdot 10^7$ Nm and $M_{xx} = -8.2 \cdot 10^7$ Nm at $t=22$ ms.

Conclusions: We report on a new method to compute the seismic point-source generated by an impact. This method relies on 3D numerical software with an ability to simulate a variety of impact scenario, including oblique impacts in various planetary surface materials. In the near future, we will test the ability of the point source representation to simulate impact-generated far-field seismic waves, and will identify possible improvements. In order to reach remote distances, we will couple the non-linear HOSS code to the elastic wave propagation software SPECFEM3D [16]. This interfacing will allow for a comparison between point-source generated signals and shock-generated signals (with finite dimensions) in the far-field, at distances relevant for seismic studies.

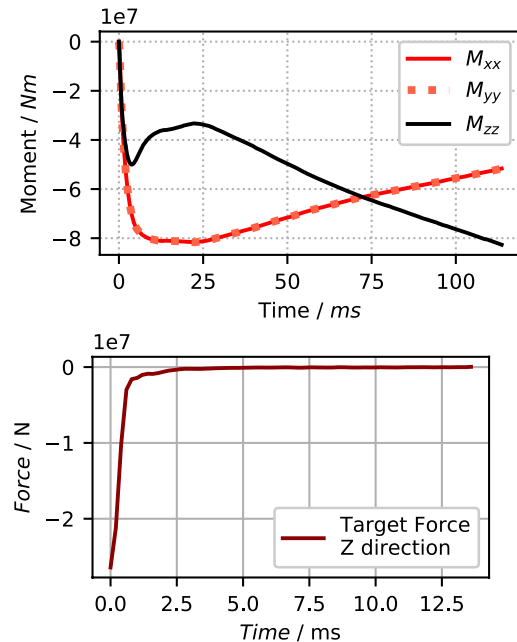


Figure 2: (top) Evolution in time of the three diagonal moment tensor components. Non-diagonal terms are zero by symmetry. (bottom) Force generated by the vertical impact in time. Note the difference in time axis between the two plots.

Acknowledgments: This work is supported by the LANL CSES and French ANR (MAGIS, ANR-19-CE31-0008-08). It uses resources provided by the LANL Institutional Computing Program. Authors are thankful to the LANL-HPC environment for developing and maintaining the Los Alamos High-Performance Computing facilities. This is LA-UR-21-20168.

References: [1] Dorman, J., S. et. al. (1978) *LPSC IV*, 3615–3626. [2] Oberst, J., & Nakamura, Y. (1987) *JGR: Solid Earth*, 92(B4), E769-E773. [3] G. Tancredi et. al. (2009) *Meteoritics & Planetary Science*, 44: 1967-1984. [4] Daubar, I. J. et al. (2020) *JGR: Planets*, 125. [5] Banerdt, W. B., et al. (2020) *Nature Geoscience*, 13, 183–189. [6] Aki, K., and Richards, P. G. (2002) *Quantitative Seismology*. [7] Munjiza, A. A. (2004) *The combined finite-discrete element method*. John Wiley & Sons. [8] Lei, Z. et al. (2014) *Computational Particle Mechanics*, 1(3), 307-319. [9] Knight, E. E. et al. (2020) *Computational Particle Mechanics*, 7(5), 765-787. [10] Backus, G., and Mulcahy, M. (1976) *GJI*, 46(2), 341-361 and 47(2), 301-329. [11] Lognonné, P., et. al. (1994). *Icarus*, 110(2), 180-195. [12] Froment, M. et al. (2020) *GRL*, 47(13). [13] Lei, Z., et al. (2020) *Computational Particle Mechanics*, 7(5), 823-838. [14] Tillotson, J. H. (1962) Report No. GA-3216, General Atomic, San Diego, CA,43. [15] Wojcicka, N. et al. (2020). *JGR: Planets*, 125(10). [16] Komatitsch, D. and Vilotte, J.P. (1998). *BSSA*, 88(2):368–392.